

# Towards unified understanding of conductance of stretched monatomic contacts

H.-W. Lee,<sup>1</sup> H.-S. Sim,<sup>2,3</sup> D.-H. Kim,<sup>4</sup> and K. J. Chang<sup>4</sup>

<sup>1</sup>Department of Physics, Pohang University of Science and Technology, Pohang, Kyungbuk 790-784, Korea

<sup>2</sup>Max-Planck-Institut für Physik komplexer Systeme, Nöthnitzer Str. 38, 01187 Dresden, Germany

<sup>3</sup>Korea Institute for Advanced Study, 207-43 Cheongryangri-dong, Dongdaemun-gu, Seoul 130-722, Korea and

<sup>4</sup>Department of Physics, Korea Advanced Institute of Science and Technology, Taejon 305-701, Korea

(Dated: November 17, 2018)

When monatomic contacts are stretched, their conductance behaves in qualitatively different ways depending on their constituent atomic elements. Under a single assumption of resonance formation, we show that various conductance behavior can be understood in a unified way in terms of the response of the resonance to stretching. This analysis clarifies the crucial roles played by the number of valence electrons, charge neutrality, and orbital shapes.

PACS numbers: 73.40.Cg, 73.40.Jn, 73.63.Rt

Monatomic contacts with one-atom-wide cross-section (referred to as “contacts” hereafter) have been realized by scanning tunneling microscopes or mechanically controllable break junctions [1]. Upon stretching, the conductance  $G$  of various contacts shows different behavior. In contacts made of monovalent atoms such as Na and Au, only one channel contributes to transport and  $G$  stays at the quantized value  $G_0 \equiv 2e^2/h$  during the stretching. [2, 3, 4, 5, 6]. In contacts made of polyvalent atoms such as Al and Pb, on the other hand, current is carried by three channels and  $G$  does not stay at quantized values during the stretching [7, 8, 9, 10]. Thus monovalent and polyvalent contacts are qualitatively different. Moreover there are differences even between polyvalent contacts; during the stretching,  $G$  increases (decreases) for Al (Pb) contacts.

The different conductance features were addressed by numerical calculations [10, 11, 12, 13, 14, 15] and some calculations reproduced experimental results for certain contacts. However the calculational results are often too specific to the particular contacts under calculation and the understanding on the origin of the aforementioned difference is yet far from satisfactory. For example, the connection between the conductance features and the number of valence electrons is poorly understood. In this respect, it is desirable to have an alternative approach that allows easier comparison of various contacts and thus provides an insightful explanation of the difference. We also remark that numerical calculations of conductance are sometimes subject to strong finite size effects [16]. Thus a naive comparison may be dangerous between experimental findings and numerical calculation results based on small cluster modelings of atomic contacts. For the behavior of Al contacts, existing calculations [10, 12] have reported qualitatively different results [17] and we suspect that the difference may be related to the finite size effect.

In this paper, we present an analysis that allows one to capture the connection between the conductance properties and microscopic features such as the number of

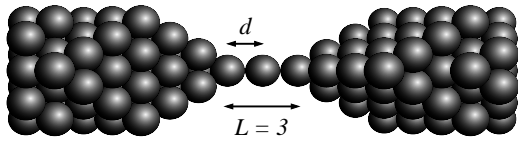


FIG. 1: A model of a monatomic Al atom contact [18].

valence electrons, charge neutrality, and orbital shapes. This connection provides a unified understanding of various conductance behavior. This analysis is applicable, provided that electron transport has resonant character.

The assumption of the resonance is very plausible in a stretched contact. First of all, the central atom of a contact (Fig. 1) [18] is relatively weakly coupled to its environment even without stretching since it has a fewer number of nearest neighbors. When stretched, the coupling becomes weaker and it is natural to expect that atomic orbitals of the central atom give rise to the resonance [19]. Among the three contacts (Na, Pb, Al) on which we are going to concentrate, the resonance formation is already demonstrated for Na and Pb contacts [10, 13, 14, 15]. For Al contacts, we present in this paper *ab initio* calculations that confirm the resonance formation.

*Transport channels.*— The number of transport channels depends on the number of valence electrons [7, 11]; while monovalent contacts have only one transport channel, polyvalent contacts have multiple channels. We begin our analysis by identifying “eigen”-transport channels, which are “eigenvectors” of a proper transmission matrix and decoupled from each other in this sense. The identification is straightforward for a contact with a symmetric shape; recent experiments [20] showed that contacts tend to align their axes with high symmetry lattice directions so that contacts have a symmetric shape. As an illustration, we describe the identification of 3 channels [11] for a (111) Al contact with the  $2\pi/3$  rotation symmetry and the inversion symmetry (Fig. 1). The rotation symmetry with respect to the  $z$ -axis (the horizontal axis in Fig. 1) makes the angular momentum  $m$

( $=0, \pm 1$ ) under the  $2\pi/3$  rotation a good quantum number. Then a traveling wave packet with a given  $m$  can be scattered into states with the same  $m$  only and thus the three eigen-transport channels of Al contacts can be characterized by  $m$ . There is a natural link between the channels and the orbitals of the central Al atom;  $m = 0$  channel couples with  $3s$  and  $3p_z$  orbitals, while  $m = \pm 1$  channels with  $3p_x \pm i3p_y$ . Here the factor  $\pm i$  implies that the two channels  $m = \pm 1$  are mutually related by the time reversal and thus degenerate.

*Friedel sum rule.*— The conductance of a contact is given by  $G = G_0 \sum_m T_m(E_F)$ , where  $T_m(E_F)$  is the transmission probability of the channel  $m$  at the Fermi energy  $E_F$ . In order to examine the connection between  $T_m$  and microscopic features, it is useful to use the Friedel sum rule [21, 22]. For a contact with the inversion symmetry, which makes the parity under the inversion a good quantum number, the Friedel sum rule [21] results in

$$T_m(E_F) = \sin^2\left(\frac{\pi}{2}\Delta N_m\right), \quad (1)$$

where  $\Delta N_m \equiv N_{m,e} - N_{m,o}$ ,  $N_{m,e(o)} = 2 \int_{E_F}^{\infty} dE \rho_{m,e(o)}(E)$ , and  $\rho_{m,e/o}$  is the density of states (DOS) with even/odd parity in the channel  $m$  (spin degeneracy assumed).

*Resonant transport and charge neutrality.*— We then examine how  $\Delta N_m$ 's are affected by microscopic features. For the resonant transport,  $\Delta N_m$  is governed by resonances,  $\Delta N_m = 2(R_{m,e} - R_{m,o})$ , where  $R_{m,e(o)}$  is the number of even (odd) parity resonances in the channel  $m$  below  $E_F$  (2 from spin degeneracy). Partially filled resonances (near  $E_F$ ) give fractional contribution to  $R_{m,e/o}$ .

Another important relation comes from the charge neutrality, which is an excellent approximation in metallic systems [13, 14]. The charge neutrality near the central atom results in  $2 \sum_m (R_{m,e} + R_{m,o}) = N'$ , where  $N'$  is the number of valence electrons in the central atom [23].

To make a further progress, we first note that  $T_m$  is periodic in  $R_{m,e/o}$  with the period 1 [Eq. (1)]. We thus ignore the integer part and focus on the fractional part of  $R_{m,e/o}$  arising from the partially filled resonance. For contacts under consideration, moreover, central atoms possess only a few atomic orbitals and as a result, there is at best one partially filled resonance in each channel. This is verified by our *ab initio* calculation given below (Al contact) and by Refs. [10, 14] (Pb and Na contacts, respectively). Then for each  $m$ , either  $R_{m,e} = 0$  or  $R_{m,o} = 0$ , and the new equality  $|\Delta N_m| = 2(R_{m,e} + R_{m,o})$  holds. The charge neutrality condition then becomes

$$\sum_m |\Delta N_m| = N'_{\text{eff}}, \quad (2)$$

where  $N'_{\text{eff}}$  can differ from  $N'$  by an integer multiple of 2 due to the neglect of the integer part of  $R_{m,e/o}$ .

*Mono. vs. polyvalent contacts.*— For monovalent contacts such as Na [14], where there is only one transport

channel and  $N' = N'_{\text{eff}} = 1$ , Eq. (2) reduces to  $|\Delta N| = 1$ . According to Eq. (1), Eq. (2) then implies  $G = G_0$  regardless of other details such as the degree of stretching, explaining the quantization of  $G$  in experiments.

In polyvalent contacts, on the other hand, there are multiple channels and multiple  $\Delta N_m$ 's. Then the single constraint (2) alone cannot completely determine  $\Delta N_m$ 's and  $G$  needs not be quantized, explaining the difference between monovalent and polyvalent contacts. This is one of the main results of this paper.

As a concrete example of polyvalent contacts, we examine the symmetric Al contact. When its central atom is weakly coupled to the electrodes, its atomic orbitals  $3s, 3p_x, 3p_y, 3p_z$  give rise to one (almost) fully occupied resonance in the  $m = 0$  channel (mostly  $s$  character) and three partially filled resonances, one in each channel. This occupation of resonances can be easily inferred from the knowledge of an isolated Al atom. When the two electrons in the fully occupied resonance are ignored,  $N'_{\text{eff}}$  is  $N' - 2 = 1$  and from Eq. (2), we have

$$|\Delta N_0| + 2|\Delta N_{\pm 1}| = 1, \quad (3)$$

where the degeneracy of the  $m = \pm 1$  channels is used. From Eq. (1), the conductance then reads

$$\frac{G}{G_0} = \sum_m T_m = \left[ \cos(\pi \Delta N_{\pm 1}) - \frac{1}{2} \right]^2 + \frac{3}{4}. \quad (4)$$

Thus  $G$  varies as  $\Delta N_{\pm 1}$  changes during the stretching.

*Orbital shapes.*— The value of  $\Delta N_{\pm 1}$  is influenced by the shapes of  $s$  and  $p$  orbitals, which make the  $pp\pi$  coupling (responsible for the partially filled  $m = \pm 1$  resonances) weaker than the  $pp\sigma$  or  $sp\sigma$  coupling (responsible for the partially filled  $m = 0$  resonance). Consequently  $|\Delta N_{\pm 1}| < |\Delta N_0|$ , and from Eq. (3), we find  $|\Delta N_{\pm 1}| < 1/3$ . The stretching magnifies the effect of the orbital shape difference [10, 24] and thus decreases  $|\Delta N_{\pm 1}|$  further below  $1/3$ . Then according to Eq. (4),  $G$  increases monotonically during the stretching, in agreement with experiments [7, 9, 10]. Our explanation for Al contacts is in qualitative agreement with Ref. [10] but differs from Ref. [12], where the displacement of the central atom from the  $z$ -axis is important. Equation (4) also predicts that  $G$  has an upper bound of  $G_0$  and a lower bound of  $0.75 G_0$ , in reasonable agreement with the histogram data [8, 25], and that  $T_0$  ( $sp$  contribution) increases during the stretching, while  $T_1$  and  $T_{-1}$  decrease. Equation (4) and its implications are the second main result of this paper.

*Pb contacts.*— Next we apply this approach to Pb contacts, where  $6p$  orbitals mediate the transport. In an isolated Pb atom, the spin-orbit coupling splits them into  $p_{1/2}$  and  $p_{3/2}$  with the former lower in energy by about 0.9 eV [26]. In a Pb contact with the  $2\pi/3$  rotational symmetry, its channels then can be classified as  $(j, m_j) = (1/2, \pm 1/2), (3/2, \pm 3/2)$ , and  $(3/2, \pm 1/2)$ , where  $j$  is the

total angular momentum and  $m_j$  is its component along the  $z$ -axis. Since each pair of channels  $(j, \pm m_j)$  are degenerate, the  $\pm$  sign can be regarded as a fictitious spin variable for the channels. Then we have three transport channels, each with the “spin” degeneracy two, and obtain  $T_{(j,|m_j|)} = \sin^2(\pi \Delta N_{(j,|m_j|)} / 2)$ , where  $\Delta N_{(j,|m_j|)} = 2 \int_{E_F}^{E_F} dE [\rho_{(j,\pm m_j),e}(E) - \rho_{(j,\pm m_j),o}(E)]$ .

Since  $N'_{\text{eff}} = 2$  for a Pb atom (2 electrons in the  $6s$  orbital are ignored), one obtains, instead of Eq. (3),

$$\sum_{(j,|m_j|)} |\Delta N_{(j,|m_j|)}| = 2. \quad (5)$$

The role of the constraint (5) becomes clear in the large  $d$  limit, where the orbital coupling to electrodes is weak and  $|\Delta N_{(3/2,3/2)}| \simeq |\Delta N_{(3/2,1/2)}| < |\Delta N_{(1/2,1/2)}|$ . Equation (5) then predicts  $T_{(3/2,3/2)} \simeq T_{(3/2,1/2)} < T_{(1/2,1/2)}$ , which agrees with a channel-resolved measurement [10]. Note that except for the difference in  $N'$  (or  $N'_{\text{eff}}$ ), Pb and Al contacts are very similar. The difference in  $N'$  is however crucial; from Eq. (5), one obtains

$$\frac{G}{G_0} \simeq \frac{9}{4} - \left[ \frac{1}{2} + \cos(\pi \Delta N_{(3/2,3/2)}) \right]^2, \quad (6)$$

which differs from Eq. (4). We next consider the behavior of  $\Delta N_{(3/2,3/2)}$ . Since the  $(3/2,3/2)$  channel is least favored by both orbital and spin-orbit couplings to electrodes,  $|\Delta N_{(3/2,3/2)}|$  should be smaller than  $2/3$  [Eq. (5)] and decay during the stretching. From Eq. (6),  $G/G_0$  then decays monotonically during the stretching with the upper (lower) bound of  $9/4$  ( $0$ ), which is in reasonable agreement with experiments [10]. For realistic values of  $d$ , on the other hand, the orbital coupling will lift the degeneracy  $|\Delta N_{(3/2,3/2)}| = |\Delta N_{(3/2,1/2)}|$ . However this effect turns out to be rather minor: A recent calculation [10] suggests that already at  $d = 1.2 d_{0,\text{Pb}}$ , where  $d_{0,\text{Pb}}$  is the bond length of bulk Pb,  $|\Delta N_{(3/2,3/2)}|$  and  $|\Delta N_{(3/2,1/2)}|$  ( $< 1$ ) are significantly smaller than  $|\Delta N_{(1/2,1/2)}|$  ( $> 1$ ). Then the predictions of Eq. (6) should remain qualitatively valid at least for  $d > 1.2 d_{0,\text{Pb}}$ . We also note that in the range of  $d$ , where  $|\Delta N_{(1/2,1/2)}| > 1$ , not only  $G$  but also each individual  $T_{(j,|m_j|)}$  decreases during the stretching due to Eq. (5). This part on Pb contacts constitutes the third main result of this paper.

*Resonance in Al contacts: Ab initio calculation.*— While the resonance formation is already verified for Na [13, 14, 15] and Pb [10] contacts, it remains rather unclear for Al contacts [27]. We thus perform first-principles calculation for an Al contact with the geometry in Fig. 1 ( $L = 3$ ). Pseudopotentials [28] and real-space multigrid method [29] within the local-density-functional approximation are used. Each electrode is modeled by a fcc cluster of  $M$  ( $= 69$ ) Al atoms. Small cluster calculations are useful to test the resonance formation although the predicted resonance positions may be wrong due to

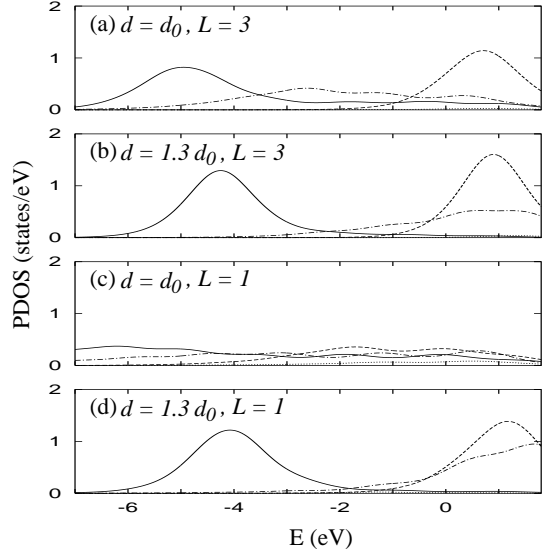


FIG. 2: Projected DOSs (PDOS) onto the central atom of Al contacts with different  $d$  and  $L$ . Solid and dash-dotted (dotted and dashed) lines represent the PDOSs for the  $m = 0$  ( $m = \pm 1$ ) channel with even and odd parity, respectively.  $E_F$  is aligned at 0 eV and the PDOS for  $m = 0$  with odd parity is magnified by factor 2 for clarity.

the finite size effect (at best  $\lesssim 1$  eV in our estimation). A supercell geometry containing the whole system is used and electrodes in neighboring supercells are separated by more than  $10.58$  Å, so that inter-supercell interactions are negligible. Using a grid spacing of  $0.44$  Å, the total energy is converged to within  $10^{-7}$  Ry. For the  $M = 69$  cluster, single particle level spacing  $\delta\epsilon$  is estimated at  $\sim 0.07$  eV near  $E_F$ . To extract properties of infinite metallic electrodes from the finite cluster calculation, the Fermi-Dirac level broadening  $E_T$  should be larger than  $\delta\epsilon$ . Using  $E_T = 0.4$  eV ( $> 3\delta\epsilon$ ), we obtain the projected DOSs (PDOS) of different  $m$  states onto a region around the central atom (a sphere with the radius of  $0.56 d_0$ ) and decompose them into even and odd parity components with respect to the inversion symmetry. Here,  $d_0$  ( $= 2.86$  Å) is the bond length of Al fcc metals.

The resonance assumption is tested for  $d = d_0$  and  $1.3 d_0$  (Fig. 2). For  $d = 1.3 d_0$ , the stretching distance is  $2(d - d_0) = 0.6 d_0$ , which is smaller than the experimental stretching distance of  $0.7 d_0$  to  $1.7 d_0$  before the contact breaking [7, 9, 10]. Figure 2(b) shows the PDOSs for  $d = 1.3 d_0$ . In the  $m = 0$  channel, two well-defined resonances develop, one with even parity (almost fully filled) and the other with odd parity. In the  $m = \pm 1$  channel, one odd parity resonance develops. Thus for  $d = 1.3 d_0$ , the resonance assumption holds for all channels. When  $d$  is reduced to  $d_0$  [Fig. 2(a)], channels respond differently due to the difference in the coupling strengths between the  $\sigma$  and  $\pi$  couplings. Whereas the resonance in the  $m = \pm 1$  channel remains well-behaved, resonances in the

$m = 0$  channel become broader and make nonnegligible overlap at  $E_F$ . Thus not all channels are in the clear resonant regime. Recalling that the resonance widths in Fig. 2 can be overestimated by  $E_T$ , we may safely conclude that Al contacts enter the clear resonant regime somewhere between  $d_0$  and  $1.3d_0$ . For  $d_0 \lesssim d \lesssim 1.3d_0$ , the correction to  $G$  from the  $m = 0$  channel being not in the clear resonant regime is  $-\sin(\pi\eta)\sin[\pi(\eta+2\Delta N_{\pm 1})]$ , where  $\eta \equiv 2 - 2R_{m=0,e}$ . Thus for  $\eta \ll 1$ , the correction is not significant and the general trend of rising  $G$  during the stretching is not altered.

The PDOSSs are calculated for the  $L = 1$  geometry model of contacts as well, where the two electrodes share a common apex atom. The PDOSSs for  $d = d_0$  [Fig. 2(c)] are essentially structureless, implying that the sharp tip geometry alone does not induce resonances at Al apex atoms, in contrast to the result for the Na (111) tip geometry [13, 14]. But the resonance assumption holds for  $d = 1.3d_0$  [Fig. 2(d)] and a conclusion similar to that for the  $L = 3$  geometry can be made.

*Discussion and conclusion.*— We first note that although contacts with a symmetric shape are used for analysis, deviations from the symmetric geometry such as disorder in atomic positions do not affect the result qualitatively, as demonstrated explicitly in Refs. [11, 13]. Secondly, our analysis can be used to study effects of  $L$  variation as well. For monovalent contacts, for example, the resonance analysis predicts different conductance behavior for even and odd  $L$  due to the difference in  $N'_{\text{eff}}$ . This prediction is consistent with the oscillation of  $G$  with  $L$  in Na contacts (first-principles calculations [14, 15]). In Au, where  $L$  is known [30] to vary during the stretching, a similar oscillation was indeed observed [6, 31], although its amplitude is smaller than the predicted value for Na probably due to the stronger coupling in Au [27]. Thirdly, our analysis can be also extended to contacts made of  $sd$  metal, which have five channels and thus could be more complex. It was recently reported [32] that a one-atom Pt contact has effectively three open channels ( $sd_{z^2}$ ,  $d_{yz}$ , and  $d_{zx}$  characters) at the Fermi level under zero bias. Here, one can find  $N'_{\text{eff}} = 4$  since 6 among 10 valence electrons of a Pt atom participate in the almost fully filled  $sd_{z^2}$ ,  $d_{xy}$ , and  $d_{x^2-y^2}$  states [32]. Then, our resonance analysis leads to  $G/G_0 \simeq 9/4 - (1/2 + \cos \pi \Delta N_{d_{yz}/d_{zx}})^2$  and  $|\Delta N_{sd_{z^2}}| + 2|\Delta N_{d_{yz}/d_{zx}}| = 4$ . Because  $|\Delta N_{d_{yz}/d_{zx}}|$  is larger than  $4/3$  and increases (at best up to 2) during the stretching [33],  $G$  decreases during the stretching with the upper bound of  $\sim 9/4G_0$ , in good agreement with Ref. [32]. Fourthly, we remark that our approach may be also useful for a wider class of systems, for example, symmetric molecules coupled to electrodes [34]. For this purpose, the charge neutrality condition (2) should be generalized to take into account possible electron transfer between molecules and electrodes arising from their electron affinity difference.

To conclude, under the single assumption of resonant

transport, it is demonstrated that qualitatively different conductance behavior in various stretched contacts can be explained in a unified way in terms of the number of electrons participating in partially filled resonance states, orbital shapes, and charge neutrality.

HSS, DHK, and KJC were supported by KISTI and QSRC at Dongkuk University, and HWL was supported by SKORE-A, eSSC, Nano Research and Development Programs, and POSTECH BSRI research fund.

- 
- [1] J. M. van Ruitenbeek, cond-mat/9910394.
  - [2] J. M. Krans, J. M. van Ruitenbeek, V. V. Fisun, I. K. Yanson, and L. J. de Jongh, *Nature (London)* **375**, 767 (1995).
  - [3] G. Rubio, N. Agrait, and S. Vieira, *Phys. Rev. Lett.* **76**, 2302 (1996).
  - [4] H. Ohnishi, Y. Kondo, and K. Takayanagi, *Nature (London)* **395**, 780 (1998).
  - [5] A. I. Yanson, G. Rubio Bollinger, H. E. van den Brom, N. Agrait, and J. M. van Ruitenbeek, *Nature (London)* **395**, 783 (1998).
  - [6] G. Rubio-Bollinger, S. R. Bahn, N. Agrait, K. W. Jacobsen, and S. Vieira, *Phys. Rev. Lett.* **87**, 026101 (2001).
  - [7] E. Scheer, P. Joyez, D. Esteve, C. Urbina, and M. H. Devoret, *Phys. Rev. Lett.* **78**, 3535 (1997); E. Scheer, N. Agrait, J. C. Cuevas, A. L. Yeyati, B. Ludoph, A. Martín-Rodero, G. R. Bollinger, J. M. van Ruitenbeek, and C. Urbina, *Nature (London)* **394**, 154 (1998).
  - [8] A. I. Yanson and J. M. van Ruitenbeek, *Phys. Rev. Lett.* **79**, 2157 (1997).
  - [9] D. Sánchez-Portal, C. Untiedt, J. M. Soler, J. J. Sáenz, and N. Agrait, *Phys. Rev. Lett.* **79**, 4198 (1997).
  - [10] J. C. Cuevas, A. Levy Yeyati, A. Martín-Rodero, G. Rubio Bollinger, C. Untiedt, and N. Agrait, *Phys. Rev. Lett.* **81**, 2990 (1998).
  - [11] J. C. Cuevas, A. Levy Yeyati, and A. Martín-Rodero, *Phys. Rev. Lett.* **80**, 1066 (1998).
  - [12] N. Kobayashi, M. Brandbyge, and M. Tsukada, *Surf. Sci.* **435**, 854 (1999); *Phys. Rev. B* **62**, 8430 (2000).
  - [13] A. Levy Yeyati, A. Martín-Rodero, and F. Flores, *Phys. Rev. B* **56**, 10369 (1997).
  - [14] H.-S. Sim, H.-W. Lee, and K. J. Chang, *Phys. Rev. Lett.* **87**, 096803 (2001); *Physica E* **14**, 347 (2002).
  - [15] S. Tsukamoto and K. Hirose, *Phys. Rev. B* **66**, 161402(R) (2002).
  - [16] J. J. Palacios, A. J. Pérez-Jiménez, E. Louis, E. San-Fabián, and J. A. Vergés, *Phys. Rev. B* **66**, 035322 (2002).
  - [17] In Ref. [10], tight-binding calculation has been performed under the constraint of the local charge neutrality. A stretched contact is modeled as a contact with enlarged atomic spacing at the contact region and it has been found that the result is in qualitative agreement with the experimental observation for Al contacts when a sufficiently large number of atomic layers from the central atom of the contact has been taken into account [13]. In Ref. [12], on the other hand, the first-principles calculation has been performed. Due to the calculational cost, only one atomic layer has been taken into account. From

- this calculation, it has been reported that the enlarged atomic spacing alone cannot explain the experimental finding and the behavior of the increasing conductance during the stretching is achieved only when the atomic arrangement at the contact region forms a “bent” wire.
- [18] It is not yet clear whether monatomic contacts in experiments correspond to the  $L = 3$  geometry in Fig. 1 or an  $L = 1$  one, where two leads share a common apex atom. Our results for both cases are the qualitatively same.
- [19] J. A. Torres and J. J. Sáenz, *Physica B* **218**, 234 (1996).
- [20] V. Rodrigues, T. Fuhrer, and D. Ugarte, *Phys. Rev. Lett.* **85**, 4124 (2000).
- [21] S. Datta and W. Tian, *Phys. Rev. B* **55**, R1914 (1997).
- [22] H.-W. Lee, *Phys. Rev. Lett.* **82**, 2358 (1999).
- [23] The charge neutrality condition may acquire a correction when the two apex atoms of the electrodes give rise to resonances. Such apex resonances are however irrelevant for atomic contacts under consideration.
- [24] D. A. Papaconstantopoulos, *Handbook of the band structure of elemental solids* (Plenum Press, New York, 1986).
- [25] These bounds can be weakly violated due to various details ignored in this idealized analysis.
- [26] K. Würde, A. Mazur, and J. Pollmann, *Phys. Rev. B* **49**, 7679 (1994).
- [27] In Ref. [24], the electron hopping energy  $\alpha$ 's (in units of eV) in Na, Au, Al, and Pb metals between neighboring atoms at their bondlengths are estimated as  $|\alpha_{ss\sigma, \text{Na}}| = 0.65$ ,  $|\alpha_{ss\sigma, \text{Au}}| = 0.91$ ,  $|\alpha_{sp\sigma, \text{Al}}| = 1.28$ ,  $|\alpha_{pp\sigma, \text{Al}}| = 2.44$ ,  $|\alpha_{pp\pi, \text{Al}}| = 0.32$ ,  $|\alpha_{sp\sigma, \text{Pb}}| = 0.75$ ,  $|\alpha_{pp\sigma, \text{Pb}}| = 1.53$ , and  $|\alpha_{pp\pi, \text{Pb}}| = 0.20$ .  $\alpha$  has the largest value for Al.
- [28] Norm-conserving pseudopotentials are generated, following N. Troullier and J. L. Martins [Phys. Rev. B **43**, 1993 (1991)], and then transformed into the separable form by L. Kleinman and D. M. Bylander [Phys. Rev. Lett. **48**, 1425 (1982)].
- [29] Y.-G. Jin, J.-W. Jeong, and K. J. Chang, *Physica* **274B**, 1003 (1999).
- [30] S. R. Bahn and K. W. Jacobsen, *Phys. Rev. Lett.* **87**, 266101 (2001); R. H. M. Smit, C. Untiedt, A. I. Yanson, and J. M. van Ruitenbeek, *Phys. Rev. Lett.* **87**, 266102 (2001); E. Z. da Silva, A. J. R. da Silva, and A. Fazzio, *Phys. Rev. Lett.* **87**, 256102 (2001).
- [31] R. H. M. Smit, C. Untiedt, G. Rubio-Bollinger, R. C. Segers, and J. M. van Ruitenbeek, condmat/0303039.
- [32] S. K. Nielsen, M. Brandbyge, K. Hansen, K. Stokbro, J. M. van Ruitenbeek, and F. Besenbacher, *Phys. Rev. Lett.* **89**, 066804 (2002).
- [33] The partially filled  $sd_{z2}$  resonance has antibonding coupling to electrodes, thus has higher energy than those of  $d_{yz}$  and  $d_{zx}$ . The details will be published elsewhere.
- [34] J. Reichert, R. Ochs, D. Beckmann, H. B. Weber, M. Mayor, and H. v. Löhneysen, *Phys. Rev. Lett.* **88**, 176804 (2002).